

Correlation for flow boiling heat transfer in mini-channels

W. Zhang^{a,1}, T. Hibiki^b, K. Mishima^{b,*}

^a Graduate School of Energy Science, Kyoto University, Kyoto 606-8317, Japan

^b Research Reactor Institute, Kyoto University, Kumatori-cho, Sennan-gun, Osaka 590-0494, Japan

Received 3 June 2004

Available online 27 September 2004

Abstract

In view of practical significance of a correlation of heat transfer coefficient in the aspects of such applications as engineering design and prediction, some efforts towards correlating flow boiling heat transfer coefficients for mini-channels have been made in this study. Based on analyses of existing experimental investigations of flow boiling, it was found that liquid-laminar and gas-turbulent flow is a common feature in many applications of mini-channels. Traditional heat transfer correlations for saturated flow boiling were developed for liquid-turbulent and gas-turbulent flow conditions and thus may not be suitable in principle to be used to predict heat transfer coefficients in mini-channels when flow conditions are liquid-laminar and gas-turbulent. By considering flow conditions (laminar or turbulent) in the Reynolds number factor F and single-phase heat transfer coefficient h_{sp} , the Chen correlation has been modified to be used for four flow conditions such as liquid-laminar and gas-turbulent one often occurring in mini-channels. A comparison of the newly developed correlation with various existing data for mini-channels shows a satisfactory agreement. In addition, an extensive comparison of existing general correlations with databases for mini-channels has also been made. © 2004 Elsevier Ltd. All rights reserved.

Keywords: Heat transfer; Flow boiling; Mini-channel; Small diameter

1. Introduction

With advance of state-of-the-art micro-scale technologies and demands for more high cooling efficiency in such practical applications as the cooling of diverters of fusion reactors, high performance electronic chips, compact heat exchangers and other heat transfer devices, research work on thermal-hydraulic characteristics of mini-channels is gaining increasing attention.

This brings up the question of channel definitions. The distinction between conventional channels, mini-channels and micro-channels is not clearly established in the literature although many related studies have been done. Based on engineering practice and application areas employing these channels, Kandlikar [1] proposed the following limits by hydraulic diameter: conventional channel (D_h larger than 3 mm), mini-channel (D_h between 200 μm and 3 mm), micro-channel (D_h between 10 and 200 μm). Mehendale et al. [2] also gave a relatively complete definition for heat exchangers in terms of hydraulic diameter. This study focuses mainly on a channel with the hydraulic diameter of the order of magnitude of the Laplace constant, or smaller than that. And we simply name it as a “mini-channel”. As well known, the Laplace length scales a bubble size and the

* Corresponding author. Tel.: +81 724 51 2449; fax: +81 724 51 2637.

E-mail addresses: wzzhang@post3.rri.kyoto-u.ac.jp (W. Zhang), hibiki@rri.kyoto-u.ac.jp (T. Hibiki), mishima@rri.kyoto-u.ac.jp (K. Mishima).

¹ Tel.: +81 724 51 2449; fax: +81 724 51 2637.

Nomenclature

Bo	boiling number, $q/(h_{fg}G)$
C	Chisholm parameter or constant in friction law
C_1-C_5	constants in the Kandlikar correlation
Co	convective number, $(1/x_{eq}-1)^{0.8}(\rho_g/\rho_f)^{0.5}$
c_p	specific heat capacity
D_h	hydraulic equivalent diameter of flow channel
dp/dz	friction pressure gradient along channel axis
F	Reynolds number factor
f	friction factor
F_f	fluid-dependent correction factor
Fr_{fo}	Froude number with all flow as liquid, $G^2/(\rho_{fg}D_h)$
G	mass flux
g	gravitational acceleration
h	heat transfer coefficient
h_{fg}	latent heat of evaporation
k	thermal conductivity
L	length from channel inlet
n	exponent in friction law
Nu	Nusselt number
p	pressure
Δp_{sat}	difference in vapor pressure corresponding to ΔT_{sat}
ΔT_{sat}	superheat, $T_w - T_{sat}$
Pr	Prandtl number
q	heat flux
Re	Reynolds number
Re_f	liquid Reynolds number, $G(1-x_{eq})D_h/\mu_f$
Re_g	gas Reynolds number, $G \cdot x_{eq}D_h/\mu_g$
S	suppression factor
T	temperature
T_m	film temperature, $(T_w + T_f)/2$
X	Martinelli parameter
x_{eq}	thermodynamic equilibrium quality

Greek symbols

β	coefficient of expansion
η	aspect ratio
μ	dynamic viscosity
ρ	density
σ	surface tension
ϕ^2	two-phase friction multiplier
ψ	heat transfer component

Superscript

'	substitute before taking maximum
---	----------------------------------

Subscripts

b	bulk liquid
cal	calculational value
Collier	Collier correlation
exp	experimental value
f	saturated liquid
fc	forced convection
fg	difference between saturated liquid and vapor
fo	all flow taken as liquid
g	saturated vapor
in	channel inlet
m	value corresponding to film temperature, T_m
nb	nucleate boiling
sat	saturated state
sp	single-phase
t	turbulent
tp	two-phase
v	laminar
w	wall

Mathematical symbols

fn	function
MAX	maximum

Taylor instability controls many crucial interfacial processes in conventional channels. Hydrodynamic phenomena governed by the Taylor instability, however, may not occur in mini-channels.

Significant differences in transport phenomena have been reported for mini-channels as compared to conventional ones [1–4,16–28]. Among various factors distinguishing flow boiling in mini-channels from that in conventional channels there are two most important to our understanding. The first one is due to the effect of surface tension. As pointed out by Mishima and Hibiki [3], the effect of surface tension becomes more important in defining the two-phase structure and bubble dynamics. Triplett et al. [4] explained that due to the dominance of surface tension, stratified flow is essentially

absent, slug (plug) and churn flow patterns occur over extensive ranges of parameters, and the slip velocity under these flow patterns is small. In such flow patterns, most of the liquid flows in a thin liquid film along the wall and the vapor flows mostly in the core of the channel due to the effect of surface tension. Since the channel size is small, it can be anticipated that at low flow rates the thin liquid flow is of characteristics of laminar flow. The second one is due to the effect of evaporation. As explained by Kandlikar [1], the effect of evaporation on flow pattern transitions is considered to be quite small in conventional channels. This is one of the reasons why the flow pattern studies on adiabatic gas–liquid systems could be extended to diabatic systems. In mini-channels, however, the effect of evaporation could

be quite significant. It alters the pressure drop characteristics. For instance, an accelerational pressure drop component could be quite large at high heat and mass fluxes due to the small channel dimension.

Traditional heat transfer coefficient correlations for saturated boiling with the liquid-turbulent and gas-turbulent flow may not be suitable in principle to predict heat transfer coefficients in mini-channels due to the possible effect of liquid flow laminarization. Therefore, the effect of the flow channel size on the flow boiling heat transfer should be carefully examined in detail. Although many analytical and experimental studies [1–4,16–28] related to flow boiling heat transfer in a mini-channel have been performed for the past decades, in the current status of this subject, sufficient systematic and accurate data bases are still unavailable to understand flow boiling characteristics in a mini-channel, and a reliable heat transfer coefficient correlation applicable to a wide range of conditions in mini-channels has not been developed yet.

For this purpose, this study is aiming at providing a literature survey of existing heat transfer correlations and the current understanding of flow boiling heat transfer characteristics in mini-channels, constructing a database, evaluating the applicability of existing correlations, and developing a heat transfer correlation for saturated flow boiling in mini-channels. The newly obtained correlation is compared with existing experimental data taken under various experimental conditions such as different channel geometries (circular and rectangular), flow orientations (vertical and horizontal), and test fluids (water, R11, R12, and R113).

2. Previous analytical and experimental works

2.1. Existing correlations for predicting saturated flow boiling heat transfer coefficients in conventional channels

In what follows, some correlations for predicting saturated flow boiling heat transfer coefficients in conventional channels will be reviewed briefly. As well known, flow boiling heat transfer is governed mainly by two important mechanisms: nucleate boiling and forced convection. So far it is not well understood yet how these two mechanisms are superimposed in the flow boiling field. Three kinds of models exist in the literature, one by Chen [5], using addition of two components corresponding to the two mechanisms with a suppression factor and a Reynolds number factor, one by Shah [6], selecting the greater one of the two components with the use of the boiling number Bo and the convective number Co , and another one by Kutateladze [7], combining two components by a power-type asymptotic model. A number of flow boiling correlations published in the last three decades are only variations of these

models. Up to now the correlations by Chen [5], Shah [6], Winterton and co-workers [8,9], Kandlikar [10], and Steiner and Taborek [11] are among the widely used correlations.

An additive concept was first suggested by Rohsenow [12] that the flow boiling heat transfers associated with forced convection and nucleate boiling could be added. By using the additive concept in principle, Chen [5] formulated the first general correlation for flow boiling heat transfer as [13]

$$h_{tp} = S \cdot h_{nb} + F \cdot h_{sp}, \tag{1}$$

where,

$$\text{for } 1/X_{tt} > 0.1, \quad F = 2.35(1/X_{tt} + 0.213)^{0.736}, \tag{2}$$

$$\text{for } 1/X_{tt} \leq 0.1, \quad F = 1, \tag{3}$$

$$h_{sp} = 0.023Re_f^{0.8}Pr_f^{0.4} \left(\frac{k_f}{D_h} \right), \tag{4}$$

$$S = 1 / (1 + 2.53 \times 10^{-6} Re_f^{1.17}), \tag{5}$$

$$h_{nb} = 0.00122 \left(\frac{k_f^{0.79} c_{pf}^{0.45} \rho_f^{0.49}}{\sigma^{0.5} \mu_f^{0.29} h_{fg}^{0.24} \rho_g^{0.24}} \right) \Delta T_{sat}^{0.24} \Delta p_{sat}^{0.75}, \tag{6}$$

$$X_{tt} = \left(\frac{1 - x_{eq}}{x_{eq}} \right)^{0.9} \left(\frac{\rho_g}{\rho_f} \right)^{0.5} \left(\frac{\mu_f}{\mu_g} \right)^{0.1}. \tag{7}$$

Here Chen introduced two dimensionless factors, the suppression factor S and the Reynolds number factor F , to account for the smaller effective superheat due to forced convection as compared to that in a pool boiling case, and for the increase in convective turbulence due to the presence of vapor phase, respectively. This correlation is widely used and taken as a benchmark in the literature.

To correlate flow boiling heat transfer coefficients Shah [6] proposed a different approach, where the nucleate boiling component was represented by the boiling number Bo , while the convective number Co was used for the forced convection component. He first used a graphical chart, later curve-fitted equations, to select the greater one of the two components, as follows:

$$\frac{h_{tp}}{h_{sp}} = \text{MAX}(\psi_{nb}, \psi_{fc}), \tag{8}$$

where the nucleate boiling component $\psi_{nb} = \text{fn}(Bo)$ and the convective component $\psi_{fc} = \text{fn}(Co)$.

His method is easy to apply because two components, nucleate boiling and forced convection, are simply represented by Bo and Co , respectively, rather than appropriate correlations. However, this simplicity restricts the range of applicability and accuracy, especially for pressure effects [11].

The correlation proposed by Gungor and Winterton [8] is a modification of the Chen correlation as follows:

$$h_{tp} = S \cdot h_{nb} + F \cdot h_{sp}, \tag{9}$$

where $S = \text{fn}(F, Re_f)$ and $F = \text{fn}(Bo, X_{tt})$. Liu and Winterton [9] pointed out the deficiencies of this correlation, and developed a new approach by using the Kutateladze power-additive model [7], as follows:

$$h_{tp} = \left[(F \cdot h_{sp,fo})^2 + (S \cdot h_{nb})^2 \right]^{1/2}, \quad (10)$$

where the Cooper pool boiling correlation [15] is used for calculation of h_{nb} .

Kandlikar [10] developed a correlation in the form of

$$h_{tp} = h_{sp}(C_1 Co^{C_2} (25 Fr_{fo})^{C_3} + C_3 Bo^{C_4} F_f). \quad (11)$$

Corresponding to the forced convection and nucleate boiling regions, respectively, two sets of constants C_1 through C_5 were established by careful regression analysis, using a large bank of water data. The heat transfer coefficient at any given condition is evaluated using the two sets of constants for the two regions, and the higher of the two heat transfer coefficient values is the choice. In addition, when tested on a refrigerant, a fluid-dependent correction factor F_f is introduced. Therefore a new factor F_f is needed when this correlation is used for any new fluid beyond the tested ones.

Steiner and Taborek [11] followed the power-type addition model proposed by Kutateladze [7] for two boiling components and built a heat transfer correlation for flow boiling based on an extensive databank.

The single-phase heat transfer coefficient, h_{sp} (or $h_{sp,fo}$), utilized in all the above-mentioned correlations, is obtained from a correlation for turbulent flow, e.g. the Dittus–Boelter correlation [14], which means the use of these correlations for laminar flow conditions in principle with some reservation.

2.2. Existing experimental works in mini-channels

Schrock and Grossman [16] conducted an experimental investigation of water flow boiling heat transfer and pressure drop in a small tube with the diameter of 2.95 mm over a wide range of pressures from 0.25 to 2.92 MPa, high mass fluxes from 1245.0 to 2939.0 kg/m²s, and heat fluxes from 306 to 2076 kW/m². Since their database included local pressure measurements and was referenced later by Chen [5] and others, it can be used as a benchmark for developing a new correlation.

Lazarek and Black [17] measured local heat transfer coefficients, pressure drops, and critical heat fluxes for saturated boiling of R113 in a round vertical tube with the inner diameter of 3.15 mm at pressures from 0.13 to 0.41 MPa, mass fluxes from 125.0 to 750.0 kg/m²s, and heat fluxes from 14 to 380 kW/m². They correlated their local heat transfer coefficient data only with the liquid Reynolds number and the boiling number since the mechanism of nucleate boiling is dominant in their experiments, as follows:

$$Nu_{tp} = 30 Re_{fo}^{0.857} Bo^{0.714}, \quad (12)$$

where $Nu_{tp} = h_{tp} D_h / k_f$, $Re_{fo} = G \cdot D_h / \mu_f$, and $Bo = q / (G \cdot h_{fg})$.

Cornwell and Kew [18] investigated the types of flow, heat transfer coefficients and pressure drops on a compact multi-channel plate. Their experimental work has led to the clear identification of three types of flow: isolated bubble, confined bubble and annular-slug flow regime. A strong relation between the flow pattern and the heat transfer coefficient was also observed in their experiment. Subsequently they [19] proposed an approach to modeling flow boiling heat transfer in mini-channels, corresponding to their proposed flow patterns. Based on the observation, they pointed out that the heat transfer to a fluid evaporating in a narrow channel might be through one of four mechanisms: (a) nucleate boiling, (b) confined bubble boiling, (c) convective boiling, and (d) partial dryout.

Wambsganss et al. [20] performed a study on boiling heat transfer of refrigerant R113 in a small diameter (2.92 mm) horizontal tube over a range of heat fluxes (9–91 kW/m²), mass fluxes (50.0–300.0 kg/m²s), and equilibrium mass qualities (0–0.9). Then, Tran et al. [21] reported some experimental investigations of flow boiling heat transfer to refrigerant R12 in a small, horizontal, rectangular channel ($D_h = 2.40$ mm), representative of flow passages in compact heat exchangers. Later, they [22] performed a similar experiment in a small circular channel ($D_h = 2.46$ mm). Subsequently, Yu et al. [23] conducted an experiment of flow boiling heat transfer to water in a small horizontal tube with the 2.98 mm inner diameter at the pressure of 0.2 MPa, and mass fluxes of 50–200 kg/m²s. A common feature of the above experiments by Wambsganss and co-workers [20–23] is that nucleate boiling is dominant in most cases, no matter what fluids (R12, R113, and water) and channel geometries (circular and rectangular) were tested. As a consequence, they reported that their data can be predicted well by the correlation of Lazarek and Black [17].

Kureta et al. [24] studied flow boiling heat transfer of water in tubes with the diameters of 2 mm and 6 mm at the atmospheric pressure and provided a database of saturated flow boiling over a range of mass fluxes from 100 to 1000 kg/m²s, heat fluxes up to 3638 kW/m². Moreover, they also investigated single-phase heat transfer in mini-channels. They found that the heat transfer may be suppressed in a small-diameter tube since vapor bubbles moves one-dimensionally in it, and as a consequence, the heat transfer enhancement due to turbulent mixing agitation by vapor bubbles may be suppressed.

Bao et al. [25] experimentally investigated flow boiling heat transfer coefficients for Freon R11 and HCFC123 in a smooth copper tube with the inner diameter of 1.95 mm. The parameter ranges examined are:

heat fluxes from 5 to 200 kW/m², mass fluxes from 50.0 to 1800.0 kg/m²s, vapor qualities from 0 to 0.9, and system pressures from 0.2 to 0.5 MPa. They found that the heat transfer coefficients were a strong function of heat flux and system pressure, while the effects of mass flux and vapor quality were very small in the ranges examined. Therefore, they concluded that the heat transfer was mainly via nucleate boiling. The correlation developed by Lazarek and Black [17] works well for their R11 data.

Lee and Lee [26] experimented flow boiling heat transfer through horizontal rectangular channels with low aspect ratios (D_h ranging from 0.78 to 3.64 mm) using R113 as a test fluid. The mass fluxes varied from 51.6 to 209.0 kg/m²s and heat fluxes were up to 16 kW/m². The uncertainties of the heat transfer coefficient ranged from $\pm 5.22\%$ to $\pm 18.1\%$ in their experiment. Their experimental conditions were similar to those by Wambsganss and co-workers [20]. However, they claimed that the flow pattern appeared to be annular and thus forced convection was dominant in their experiment, contrary to what Wambsganss and co-workers concluded. They correlated their data, in the range of $Re_f \leq 200$, only by using the forced convection component in the Chen correlation but with a modified form of the Reynolds number factor F , which is a function of the two-phase multiplier ϕ_r^2 , and a geometry parameter. For other data with $Re_f > 200$, they reported the Kandlikar correlation works well.

Sumith et al. [27] surveyed flow boiling heat transfer of water experimentally in a vertical tube with the 1.45 mm diameter, which is less than the Laplace constant, under the atmospheric pressure over a range of mass fluxes from 23.4 to 152.7 kg/m²s, heat fluxes from 10 to 715 kW/m² and qualities up to 0.8. Large heat transfer enhancement was observed and existing flow boiling correlations largely under-predicted the heat transfer coefficients especially for the low heat flux conditions lower than 200 kW/m². The under-prediction gradually decreased with increasing heat flux. The dominant flow pattern in the tube was slug-annular or annular flow, and consequently the liquid film evaporation was found to be dominant in heat transfer.

Qu and Mudawar [28] measured saturated flow boiling heat transfer in a water-cooled three-side-heating micro-channel heat sink with 21 parallel channels having a $231 \times 713 \mu\text{m}$ cross-section over a mass velocity range of 135–402 kg/m²s, inlet temperatures of 30 and 60 °C, and an outlet pressure of 0.117 MPa. Their results indicated an abrupt transition to annular flow near the point of zero thermodynamic equilibrium quality, and revealed the dominant heat transfer mechanism is forced convection corresponding to annular flow. Contrary to trends in conventional channels, the heat transfer coefficient was shown to decrease with increasing thermodynamic equilibrium quality. Then they introduced an

annular flow model with droplet entrainment and deposition effects to predict the observed unique tendency.

3. Results and discussion

3.1. Databases used to develop correlation for saturated flow boiling heat transfer in mini-channels

All available datasets for saturated flow boiling heat transfer in mini-channels were shown in Table 1. There are 13 collected datasets and 1203 data points in our collected databank, covering a wide range of system pressures from 0.101 to 1.21 MPa, mass fluxes from 23.4 to 2939 kg/m²s, heat fluxes from 2.95 to 2511 kW/m², and hydraulic diameters of channels from 0.78 to 6.00 mm. The test fluids include water, and refrigerants (R11, R12 and R113), flowing in a single circular or rectangular channel at the condition of vertical or horizontal flow orientation.

Fig. 1 shows all collected data in the form of the liquid Reynolds number against the gas Reynolds number. Symbols used for each database are depicted in Table 1 and are common in Figs. 1–3. Four flow conditions are divided as Lockhart and Martinelli [29]. When $Re_f < 1000$ and $Re_g < 1000$ (condition vv), both liquid and gas flows are laminar. There are only 19 data points belonging to this condition. When $Re_f > 2000$ and $Re_g < 1000$ (condition tv), the liquid flow is turbulent whereas the gas flow is laminar. Fig. 1 shows there are only four data. When $Re_f < 1000$ and $Re_g > 2000$ (condition vt), the liquid flow is laminar whereas the gas flow is turbulent. Most of our collected data is located in this condition. In total, there are 716 data points falling into this condition. Since most of existing experimental investigations on mini-channels used low mass fluxes and small hydraulic diameters, the Reynolds numbers for each phase are small from their definitions. The low Reynolds number is an important indicator of flow laminarization in a mini-channel. When $Re_f > 2000$ and $Re_g > 2000$ (condition tt), both liquid and gas flows are turbulent. All the data from Schrock and Grossman [16] are located in this condition. There are 288 data points falling into this condition. The corresponding forms of the Martinelli parameter (X_{vv} , X_{tv} , X_{vt} , and X_{tt}) and values of the Chisholm parameter C for each condition are also shown in Fig. 1. The hatched parts are transition regions between the defined conditions by Lockhart and Martinelli [29]. The values of the Martinelli parameter and the Chisholm parameter can be determined by an interpolation method.

3.2. Comparison of existing correlations with collected data for mini-channels

There are the following six heat transfer correlations for saturated flow boiling frequently used in the

Table 1
Collected database for saturated flow boiling heat transfer in mini-channels

Symbol	Reference	Fluid	D_h (mm)	p (MPa)	G (kg/m ² s)	q (kW/m ²)	Orientation of flow	Geometry	Point number
○	Sumith et al. [27]	Water	1.45	0.101	23.4–153	32.0–715	Vertical upflow	Circular	161
◻	Kureta et al. [24]	Water	2.00	0.101	500, 1000	402–2302	Vertical upflow	Circular	8
▽	Schrock and Grossman [16]	Water	2.95	0.290–1.21	1245–2939	306–2076	Vertical upflow	Circular	173
◇	Yu et al. [23]	Water	2.98	0.200	103	5.00–163	Horizontal	Circular	35
⊖	Kureta et al. [24]	Water	6.00	0.101	100, 500, 1000	151–2511	Vertical upflow	Circular	43
▽	Bao et al. [25]	R11	1.95	0.294–0.470	167–560	52.0–125	Horizontal	Circular	82
○	Tran et al. [21,22]	R12	2.40 (1.70 × 4.06)	0.825–0.866	54.6–396	4.10–33.7	Horizontal	Rectangular	97
◻	Tran et al. [22]	R12	2.46	0.825	63.3–300	7.50–59.4	Horizontal	Circular	61
◇	Lee and Lee [26]	R113	0.780 (0.400 × 20.0)	0.101	104–209	2.98–10.0	Horizontal	Rectangular	91
△	Lee and Lee [26]	R113	1.90 (1.00 × 20.0)	0.101	51.6–208	2.95–15.0	Horizontal	Rectangular	179
⊖	Wambsganss et al. [20]	R113	2.92	0.124–0.160	50.0–300	8.80–90.8	Horizontal	Circular	90
◇	Lazarek and Black [17]	R113	3.15	0.170	502	64.0–178	Vertical up and down flow	Circular	14
▷	Lee and Lee [26]	R113	3.63 (2.00 × 20.0)	0.101	51.7–182	4.52–15.8	Horizontal	Rectangular	169
	Total	Water, R11, R12, R113	0.780–6.00	0.101–1.21	23.4–2939	2.95–2511	Vertical, Horizontal	Circular, Rectangular	1203

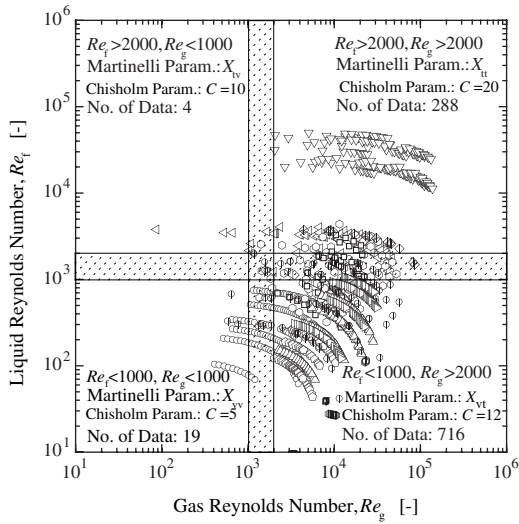


Fig. 1. Distribution of existing data points for mini-channels in four conditions.

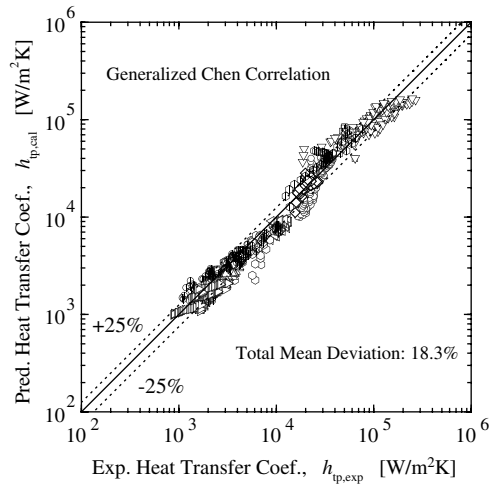


Fig. 3. Comparison of prediction by generalized Chen correlation with all data.

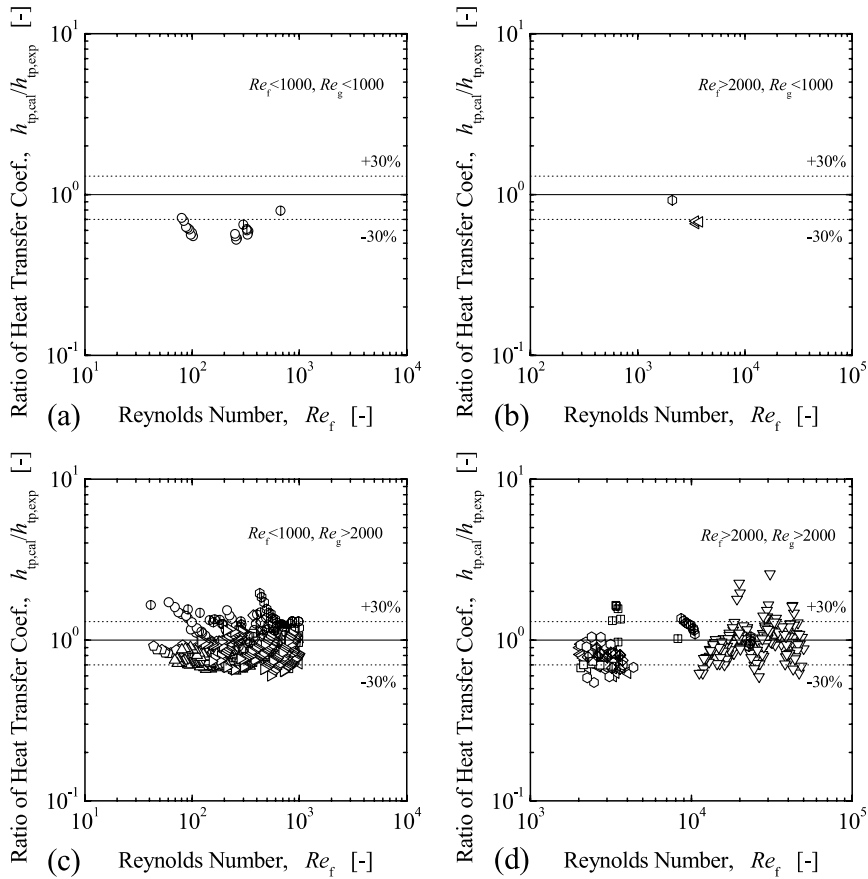


Fig. 2. Comparison of prediction by generalized Chen correlation with data in (a) liquid-laminar and gas-laminar condition, (b) liquid-turbulent and gas-laminar condition, (c) liquid-laminar and gas-turbulent condition, (d) liquid-turbulent and gas-turbulent condition.

literature: the correlations by Chen [5], Shah [6], Gungor–Winterton [8], Kandlikar [10], Liu–Winterton [9], and Steiner–Taborek [11]. Here an extensive comparison is made for these existing correlations with 13 datasets taken in mini-channels. It should be noted that all these existing correlations are extendedly used out of their applicable ranges in the original forms with the Dittus–Boelter-type correlations for turbulent flow although physically it may not be consistent with the flow conditions of vv, tv and vt. The comparison results are shown in Table 2. The mean deviation defined below the table is used as a measure of predictive accuracy. The underlined figures in the table are the smallest mean deviation among all by the existing correlations. In general, the Chen correlation gives the best predictive accuracy of 20.1% among the six existing correlations. The second is the Liu–Winterton with a mean deviation of 21.8%, followed subsequently by the Kandlikar with 23.2%, the Shah with 26.6%, the Gungor–Winterton with 37.3% and Steiner–Taborek with 66.0% finally. As for five databases using water as a test fluid, the Liu–Winterton correlation presents the best predictive behavior among six existing correlations with the four smallest mean deviations. The second is the Chen. The Steiner–Taborek correlation failed to give a reasonable prediction for Sumith’s database due to the ineffectiveness of the built-in single-phase heat transfer correlation when $Re_f < 1000$. As for the other eight databases using refrigerants (R11, R12, and R113) as test fluids, the Chen correlation shows the best predictive behaviors among six existing correlations with four smallest mean deviations. The second is the Liu–Winterton, followed by the Kandlikar, the Shah, the Gungor–Winterton and the Steiner–Taborek subsequently. The Steiner–Taborek correlation also failed to predict the Lee data for a channel with the hydraulic diameter of 0.78 mm.

From the above comparison, it is concluded that the Chen correlation gives the best prediction accuracy among the six existing correlations in total for this collected databank. For datasets using refrigerants as test fluids, the Chen correlation is also the best whereas the Liu–Winterton correlation works best when water is used as a test fluid. The Chen, Liu–Winterton and Kandlikar correlations could be recommended for use under tt conditions in mini-channels. It should be also emphasized here that large deviations from some correlations are not necessarily related to weaknesses in the correlations themselves, but more to the operating conditions of the datasets falling outside the recommended applicable ranges for most correlations.

3.3. Development of correlation for saturated flow boiling heat transfer in mini-channels

From the comparison in the last section, it is clear that the Chen correlation still works the best among

the six tested correlations although most of the collected databases are out of its applicable ranges. In addition, from the viewpoint of physical mechanisms it is still the most reasonable one in the literature so far, although other correlations may also give good predictions based on the regression analysis of a large amount of databases. Since the Chen correlation was developed for tt conditions, it may not be consistent to use it under other flow conditions. For this reason, the present study is aiming at providing a general and physically sound approach to extend its use to other flow conditions.

3.3.1. Applicability of Chen correlation for flow boiling heat transfer in mini-channels

As already shown in Section 3.1, most of the existing data taken in mini-channels fall into vt conditions instead of tt conditions in which the datasets used in developing the Chen correlation were located. As a consequence, the applicability of the Chen correlation should be evaluated physically again if applied for flow boiling heat transfer in mini-channels. In addition, this correlation was based on the assumption that two-phase flow convective heat transfer could be described by the Dittus–Boelter type equation. The validity of this assumption is quite questionable when used for other conditions since the Dittus–Boelter equation is applicable only for turbulent flow. Therefore, the whole forced convection component, consisting of the terms of the single-phase heat transfer coefficient h_{sp} and the factor F , should be changed when applied for other flow conditions.

As for the nucleate boiling component in the Chen correlation, since the nucleate boiling mechanism could be dominant for flow boiling in a mini-channel as observed in many experiments [17,20–23,25], bubble nucleation can still occur in it and thus the similar nucleate boiling mechanism as pool boiling can also be assumed. As a consequence, the correlation by Forster and Zuber [30], Eq. (6), may still be valid to predict the nucleate boiling heat transfer coefficient h_{nb} . The suppression factor, S , defined as the ratio of the effective superheat to the total wall superheat, can be expressed as a function of the local two-phase Reynolds number, and it approaches to unity at the flow rate of zero. In mini-channels, it is postulated that the bubble nucleate situation may be similar to that in pool boiling system when the two-phase Reynolds number is small. For this reason, the real suppression factor should also approach unity, in accordance with the tendency in the Chen correlation. Therefore, we assume here that the factor S in the Chen correlation may still be applicable for other conditions.

3.3.2. Modification of Reynolds number factor F

It was pointed out in the preceding section that the Chen correlation is inconsistent when used for other flow conditions than turbulent–turbulent (tt) one, since

Table 2
Comparison of correlations with datasets

Symbol	First author	D_h (mm)	Fluid	Orientation ^a	Data points	Mean deviation ^b (%)						
						Shah	Gungor–Winterton	Kandlikar	Liu–Winterton	Steiner–Taborek	Chen	Present study
○	Sumith	1.45	Water	V	161	40.7	59.6	31.6	<u>22.3</u>	–	25.5	18.3
◻	Kureta	2.00	Water	V	8	77.1	118.7	59.7	35.9	40.1	42.0	36.6
▽	Schrock	2.95	Water	V	173	18.6	25.3	17.1	22.9	27.2	15.9	18.1
◇	Yu	2.98	Water	H	35	36.3	48.2	37.9	8.6	46.4	43.4	10.7
⊕	Kureta	6.00	Water	V	43	67.1	65.4	29.9	17.0	25.4	37.1	28.6
△	Bao	1.95	R11	H	82	11.3	47.0	26.0	24.8	138.1	25.6	23.9
⊙	Tran	2.40	R12	H	97	41.8	15.1	28.4	31.2	92.6	14.4	16.1
◻	Tran	2.46	R12	H	61	37.9	22.6	22.7	24.8	108.0	<u>17.0</u>	13.5
◊	Lee	0.780	R113	H	91	20.5	20.5	19.8	<u>19.7</u>	–	24.7	16.0
△	Lee	1.90	R113	H	179	19.4	28.4	20.6	24.1	49.6	16.7	20.3
⊕	Wambsganss	2.92	R113	H	90	25.3	74.5	29.5	<u>23.7</u>	152.4	24.7	18.3
⊕	Lazarek	3.15	R113	V	14	7.7	59.5	31.1	20.1	92.2	20.9	21.5
▽	Lee	3.63	R113	H	169	14.4	25.1	11.4	13.2	43.3	9.6	16.1
Total						26.6	37.3	23.2	21.8	66.0	<u>20.1</u>	18.3

^a V: vertical, H: horizontal.

^b Mean deviation is defined as $(1/N) \sum |(h_{tp,exp} - h_{tp,cal})/h_{tp,exp}| \times 100\%$, bold figures denote the smallest mean deviation among all including the present study, and underlined figures are the smallest among all except the present study.

the two-phase forced convection heat transfer is described based on the Dittus–Boelter correlation which was originally developed for a turbulent flow. For a laminar flow, especially in mini-channels in which flow laminarization is important, some new approach should be made taking account of flow conditions. Therefore, the forced convection component in the Chen correlation, consisting of h_{sp} and F should be reexamined. In what follows, the Reynolds number factor in the Chen correlation will be reexamined and modified for use to other flow conditions.

Since the Reynolds number factor F is introduced to account for the increase in convective turbulence due to the presence of vapor phase, it should be related to the two-phase friction multiplier. Note that the right-hand-side of Eq. (2) can be approximated as

$$F = 2.35(1/X_{tt} + 0.213)^{0.736} \approx 0.64(1 + 20/X_{tt} + 1/X_{tt})^{0.5}. \quad (13)$$

Since the two-phase friction multiplier, $\phi_{f,tt}^2$, according to Chisholm [31], can be expressed by

$$\phi_{f,tt}^2 = 1 + \frac{20}{X_{tt}} + \frac{1}{X_{tt}^2}, \quad (14)$$

the Reynolds number factor can then be expressed in terms of the two-phase friction multiplier as

$$F \approx 0.64(\phi_{f,tt}^2)^{0.5} = 0.64\phi_{f,tt}, \quad (15)$$

namely,

$$F' = 0.64(\phi_{f,tt}^2)^{0.5} = 0.64\phi_{f,tt}, \quad (16)$$

where F' denotes the approximation of F and is used temporarily as the substitute of factor F . Noting that the conditions in Eqs. (2) and (3), namely, the factor F in the Chen correlation should be larger than unity, combining Eq. (16) with Eq. (3) leads to

$$F = \text{MAX}(F', 1), \quad (17)$$

which is easier to be used in computer programming and has the same function as Eqs. (2) and (3).

From the above recast, it is found that the Reynolds number factor F in Chen correlation is actually proportional to the factor $\phi_{f,tt}$ for tt flow condition. The essential aspect of the Reynolds number factor F in Chen correlation is an analogy of the root of the two-phase multiplier, $\phi_{f,tt}$. To extend the applicable ranges of the Chen correlation, it may be reasonably assumed the relationship between the Reynolds number factor F and the root of the two-phase multiplier ϕ_f holds for other flow conditions. Therefore, Eq. (16) may be recast again by a general form for four conditions according to Chisholm [31], as follows:

$$F' = 0.64(\phi_f^2)^{0.5} = 0.64\phi_f, \quad (18)$$

$$\phi_f^2 = 1 + \frac{C}{X} + \frac{1}{X^2}, \quad (19)$$

where, according to Lockhart and Martinelli [29], the definition of the Martinelli parameter X is given by

$$X^2 \equiv \frac{(dp/dz)_f}{(dp/dz)_g}, \quad (20)$$

and the values of Chisholm parameter C are given in Fig. 1 in terms of Re_f and Re_g (for the hatched parts in Fig. 1, an interpolation can be applied to obtain the values of C). Since the single-phase frictional pressure drops for liquid phase and gas phase can be represented, respectively, by

$$\left(\frac{dp}{dz}\right)_f = \frac{2f_f}{D_h} \cdot \frac{G^2(1-x_{eq})^2}{\rho_f} \quad (21)$$

and

$$\left(\frac{dp}{dz}\right)_g = \frac{2f_g}{D_h} \cdot \frac{G^2x_{eq}^2}{\rho_g}, \quad (22)$$

the Martinelli parameter X can be denoted by

$$X = \left(\frac{f_f}{f_g}\right)^{0.5} \left(\frac{1-x_{eq}}{x_{eq}}\right) \left(\frac{\rho_g}{\rho_f}\right)^{0.5}. \quad (23)$$

Lockhart and Martinelli [29] assumed the following friction law to be used for both liquid phase and gas phase in Eq. (23):

$$f_k = C_k \cdot Re_k^{-n}, \quad (k = f \text{ or } g), \quad (24)$$

where, for laminar flow in a circular channel ($Re_k < 1000$) $C_k = 16$ and $n = 1$, whereas for turbulent flow ($Re_k > 2000$) $C_k = 0.046$ and $n = 0.20$.

However, for laminar flow in a rectangular channel ($Re_k < 1000$), the following equation [32] may be more appropriate:

$$f_k = \frac{24}{Re_k} (1 - 3.55\eta + 1.947\eta^2 - 1.701\eta^3 + 0.956\eta^4 - 0.254\eta^5), \quad (25)$$

where η represents the aspect ratio, defined as the ratio of the height with the width of channel cross-section.

For $1000 \leq Re_k \leq 2000$, friction factors can be obtained by an interpolation method.

It should be noted here that selection of a friction-factor correlation for laminar flow is flexible in our approach and should depend on the channel geometry, boundary conditions and so on. For other cases, an appropriate correlation may be found in related textbooks. All modifications of the Reynolds number factor are listed in Table 3.

The reason why the Reynolds number factor could be correlated by the two-phase friction multiplier ϕ_f^2 may be simply explained by the Fanning-type friction-pres-

Table 3
Summary of generalized Chen correlation

Basic equation: $h_{tp} = S \cdot h_{nb} + F \cdot h_{sp}$	
S	$S = 1 / (1 + 2.53 \times 10^{-6} Re_f^{1.17})$
h_{nb}	$h_{nb} = 0.00122 \left(\frac{k_f^{0.79} c_{pf}^{0.45} v_g^{0.24}}{\sigma^{0.5} \mu_f^{0.29} h_{fg}^{0.24} v_f^{0.49}} \right) \Delta T_{sat}^{0.24} \Delta P_{sat}^{0.75}$
F	<p>$F = \text{MAX}(F', 1)$, $F' = 0.64 \phi_f$, $\phi_f^2 = 1 + \frac{C}{X} + \frac{1}{X^2}$ For $Re_f < 1000$ and $Re_g < 1000$, $X = X_{vv}$, $C = 5$; For $Re_f > 2000$ and $Re_g < 1000$, $X = X_{iv}$, $C = 10$; For $Re_f < 1000$ and $Re_g > 2000$, $X = X_{vt}$, $C = 12$; For $Re_f > 2000$ and $Re_g > 2000$, $X = X_{vv}$, $C = 20$; For other regions of Re_k, ($k = f$ or g), interpolate the above values of C.</p> $X = \left[\frac{\left(\frac{dp}{dz}\right)_f}{\left(\frac{dp}{dz}\right)_g} \right]^{1/2} = \left(\frac{f_f}{f_g} \right)^{0.5} \left(\frac{1 - x_{eq}}{x_{eq}} \right) \left(\frac{\rho_g}{\rho_f} \right)^{0.5}$ <p>The follow equations are applicable to both phases (liquid and gas):</p> $f_k = \begin{cases} 16/Re_k, & \text{for circular channel and } Re_k < 1000; \\ \frac{24}{Re_k} (1 - 3.55\beta + 1.947\beta^2 - 1.701\beta^3 + 0.956\beta^4 - 0.254\beta^5), & \text{for } Re_k < 1000 \text{ in rectangular channel;} \\ 0.046Re_k^{-0.2}, & \text{for } Re_k > 2000; \end{cases}$ <p>For $1000 \leq Re_k \leq 2000$, interpolate the above values of f_k.</p>
h_{sp}	<p>$Nu'_{sp,v} = 4.36$ for circular channel; $Nu_{sp,t} = 0.023Re_f^{0.8} Pr_f^{0.4}$; $Nu'_{sp,v} = 8.235(1 - 2.042\beta + 3.085\beta^2 - 2.4765\beta^3 + 1.058\beta^4 - 0.186\beta^5)$ for rectangular channel;</p> $Nu_{Collier} = 0.17Re_f^{0.33} Pr_f^{0.43} \left(\frac{Pr_f}{Pr_w} \right)^{0.25} \left\{ \frac{g \cdot \beta \cdot \rho_f^2 \cdot D_h^3 (T_w - T_f)}{\mu_f^2} \right\}^{0.1};$ $h_{sp} = \begin{cases} \frac{k_f}{D_h} \text{MAX}(Nu'_{sp,v}, Nu_{Collier}), & \text{if } Re_f \leq 2000 \text{ for vertical flow;} \\ \frac{k_f}{D_h} \text{MAX}(Nu'_{sp,v}, Nu_{sp,t}), & \text{if } Re_f < 2300 \text{ for horizontal flow;} \\ \frac{k_f}{D_h} Nu_{sp,t}, & \text{if } Re_f \geq 2300 \text{ for both vertical and horizontal flows;} \end{cases}$ <p>For vertical flow at $2000 < Re_f < 2300$, interpolate the values of h_{sp} for vertical flow at $Re_f = 2000$ and $Re_f = 2300$.</p>

sure-drop equations such as Eqs. (21) and (22). For liquid-phase flow, Eq. (21) with Eq. (24) leads to

$$\left(\frac{dp}{dz} \right)_f \approx \text{fn}(Re_f). \tag{26}$$

For two-phase flow, provided that the homogeneous model and the Fanning-type pressure-drop equation could be applied, the following relationship could be obtained:

$$\left(\frac{dp}{dz} \right)_{tp} \approx \text{fn}(Re_{tp}). \tag{27}$$

From Eqs. (26) and (27), it can be obtained

$$\frac{(dp/dz)_{tp}}{(dp/dz)_f} \equiv \phi_f^2 \approx \text{fn} \left(\frac{Re_{tp}}{Re_f} \right). \tag{28}$$

On the other hand, it is recognized that the Reynolds number factor F in the Chen correlation was deduced in the similar way and is a function of Reynolds numbers as follows

$$F = \left(\frac{Re_{tp}}{Re_f} \right)^{0.8}. \tag{29}$$

Therefore, from Eqs. (28) and (29), it can be reasonably obtained that the Reynolds number factor F may be a function of the two-phase friction multiplier ϕ_f^2 .

3.3.3. Modification of single-phase heat transfer correlation

Since the Dittus–Boelter correlation, Eq. (4), is developed for single-phase turbulent flow and its applicable range is $10^4 \leq Re_f \leq 10^5$ and $1 \leq Pr_f \leq 10$, it may not be suitable to predict single-phase heat transfer coefficients when flow is laminar, especially in mini-channels. For this reason, it would be better to replace it by single-phase laminar flow equations, as follows:

For a circular channel under uniform heat flux conditions:

$$Nu'_{sp,v} = 4.36. \tag{30}$$

For rectangular channel under uniform heat flux conditions, the simplified equation proposed by Hartnett and Kostic [32] can be used, as follows:

$$Nu'_{sp,v} = 8.235(1 - 2.042\eta + 3.085\eta^2 - 2.4765\eta^3 + 1.058\eta^4 - 0.186\eta^5). \tag{31}$$

Two sets of correlations are selected in terms of flow orientation due to the difference in the effect of gravity. First, for vertical channels, when $Re_f \leq 2000$, in order to take account of the effect of mixed convection, the following equations can be used to evaluate single-phase heat transfer coefficients [33].

$$Nu_{sp,v} = \text{MAX}\left(Nu'_{sp,v}, Nu_{\text{Collier}}\right), \quad (32)$$

where Nu_{Collier} is given by [34]

$$Nu_{\text{Collier}} = 0.17Re_f^{0.33}Pr_f^{0.43}\left(\frac{Pr_f}{Pr_w}\right)^{0.25} \times \left\{ \frac{g \cdot \beta \cdot \rho_f^2 \cdot D_h^3 (T_w - T_f)}{\mu_f^2} \right\}^{0.1}. \quad (33)$$

Here β is the expansion coefficient of liquid phase and $\beta = (\rho_f - \rho_m)/[\rho_m(T_m - T_f)]$. When $Re_f \geq 2300$, for simplicity, the following Dittus–Boelter correlation could be utilized,

$$Nu_{sp,t} = 0.023Re_f^{0.8}Pr_f^{0.4}. \quad (34)$$

In the region of $2000 < Re_f < 2300$, a linear interpolation in log scales between Eqs. (32) and (34) can be employed, as follows:

$$Nu_{sp,tr} = \left(Nu_{ve}^{\frac{\log Re_{tb}}{\log Re_{tb} - \log Re_{ve}}} / Nu_{tb}^{\frac{\log Re_{ve}}{\log Re_{tb} - \log Re_{ve}}} \right) \cdot Re_f^{\frac{\log Nu_{tb} - \log Nu_{ve}}{\log Re_{tb} - \log Re_{ve}}}, \quad (35)$$

where $Re_{ve} = 2000$, $Re_{tb} = 2300$, Nu_{ve} denotes $Nu_{sp,v}$ at Re_{ve} , and Nu_{tb} represents $Nu_{sp,t}$ at Re_{tb} .

Second, for horizontal channels, when $Re_f \geq 2300$, the Dittus–Boelter correlation, Eq. (34), could be applied. Considering the laminar flow developing length from channel inlet is usually longer than that of turbulent flow, and each phase in flow boiling system is never fully developed, the following simple equation may be appropriate in the region of $Re_f < 2300$.

$$Nu_{sp,v} = \text{MAX}\left(Nu'_{sp,v}, Nu_{sp,t}\right). \quad (36)$$

It should also be noted that, selection of the heat transfer correlation for laminar flow, as in the case of the laminar flow friction factor, is flexible in our approach and should depend on the channel geometry, boundary conditions, channel length and so on. The above correlations were selected for this collected database. All modifications of the single-phase heat transfer correlations are listed in Table 3. For other cases, an appropriate correlation may be found in related textbooks.

3.4. Comparison of generalized Chen correlation with experimental data

3.4.1. Comparison with all experimental data

In this section, the generalized Chen correlation is evaluated by the existing data listed in Table 1. First, the newly developed correlation is compared with all data for each condition to show the whole behaviors of prediction. Fig. 2(a)–(d) show in turn the comparison results for vv, tv, vt and tt conditions. The results shown in Fig. 2 are in the form of the ratio of the heat transfer coefficient predicted by the generalized correlation to the experimental value as a function of the liquid Reynolds number. Although very few experimental data points are located in vv and tv conditions, it is also useful to check the behaviors of the correlation for these conditions. The mean deviations are around 30%, and there are no systematic prediction errors by the generalized correlation. As for a channel with the inner diameter of 1.45 mm, this may not be a bad result, as shown in Fig. 2(a) and (b). For these two conditions, more data and further experimental investigations will be needed to verify the correlation. Fig. 2(c) shows the comparison results for vt conditions. It indicates that most of the predictions by the correlation are within the error bands of $\pm 30\%$ and there are no significant systematic tendencies observed. Even for a channel with the hydraulic diameter of 0.780 mm, most of predictions fall into the error bands of $\pm 30\%$. Considering large measurement errors in experiments of mini-channels, different geometries, flow orientations and test fluids, the prediction results appear to be reasonably good for all data in this condition. Fig. 2(d) shows the comparison results in tt condition. Actually, since only a recast of the Reynolds number factor F in the original Chen correlation has been made, the generalized Chen correlation should work as well as the original one. To check the validity of the recast, a database obtained by Schrock and Grossman [16] was also included in our collected database, which was originally used in the development of the Chen correlation. The predictions of the correlation for the database by Schrock and Grossman are well centered and within the $\pm 30\%$ error bars. This means our recast of the Reynolds number factor F is successful. A small part of experimental data taken from mini-channels in recent years are also located in this condition and can be predicted very well by the generalized correlation. This further indicates the successful recast, although the good prediction behaviors in this tt condition are almost completely due to the original Chen correlation. Table 2 shows in detail the comparison of the generalized Chen correlation with the six existing correlations for each database. Bold figures in the table denote the smallest mean deviation of prediction among all including the present work. For four databases, the generalized Chen correlation works best. The database

by Lee for a channel with the smallest hydraulic diameter of 0.780 mm in our databank is best predicted by the generalized correlation. The database taken by Sumith for water flow boiling in a tube with the diameter of 1.45 mm is also best predicted by the generalized correlation. Eight among 13 databases are predicted within the accuracy of 20%. In total, the generalized correlation gives the smallest mean deviation of 18.3% among all as well. The total prediction behavior of the generalized Chen correlation for all collected data under the four conditions is shown in Fig. 3. The heat transfer coefficients spanning almost three orders of magnitude are well predicted within $\pm 25\%$ error bars. Although the prediction of the newly developed correlation could not improve predictive accuracy much from the original Chen correlation for the existing data in mini-channels, actually this work generalized the Chen correlation for the four flow conditions, provided a physically sound approach to predict flow boiling heat transfer in mini-channels without bringing in any empirical constants, gave an general analogy of the Reynolds number factor in the Chen correlation to the root of the two-phase friction multiplier, and connected the prediction of heat transfer coefficient tightly with that of pressure drop.

3.4.2. Comparison with boiling curves

In what follows, the predictions by the new correlation are compared with boiling curves available in some databases. Since most of databases are given in the figures of h_{tp} versus x_{eq} with some system parameters, enough information for boiling curves could not be available. On the other hand, owing to nucleate boiling mechanism dominant in many experiments [17,20–23,25], the effect of mass flux on boiling curves is not clear in those experiments. Therefore only boiling curves obtained by Kureta et al. [24] and Sumith et al. [27] are presented here. Three typical datasets taken at different mass fluxes by Kureta et al. were shown in Figs. 4–6. Since their database also included the single-phase heat transfer data, it may be useful to check the validity of the single phase heat transfer correlations used in the generalized correlation and thus the figures are shown in the form of heat flux against wall temperature instead of wall superheat. The figures indicate that the correlations for single-phase flow built in the generalized correlation can predict single-phase heat transfer coefficients in mini-channels reasonably well. This makes the newly developed correlation physically sounder to be applied in mini-channels. From Figs. 4–6, it can be observed that the curve in the nucleate boiling region moves towards higher wall temperature with increasing mass fluxes from 100 to 1000 kg/m²s. This tendency is more remarkable at higher qualities and mass fluxes. This may be due to the effect of local pressure. As pointed out by Kandlikar [1], in mini-channels, the effect of evaporation could be quite significant. It alters the pres-

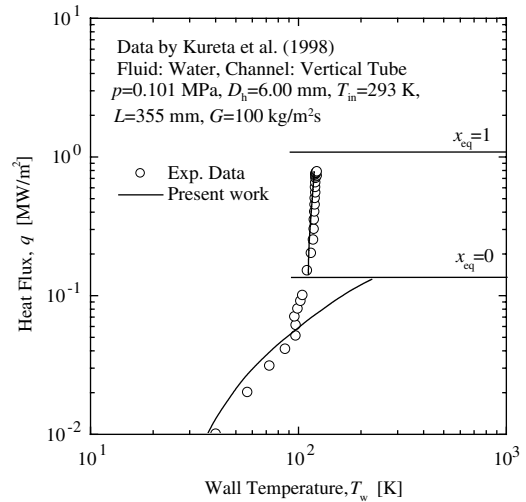


Fig. 4. Comparison with boiling curve at mass flux of 100 kg/m²s [24].

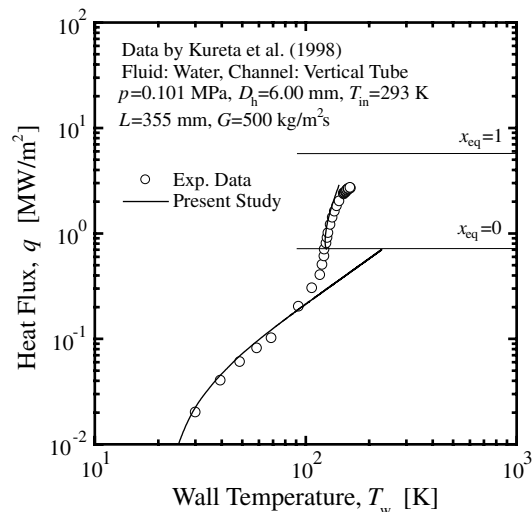


Fig. 5. Comparison with boiling curve at mass flux of 500 kg/m²s [24].

sure drop characteristics by introducing an acceleration pressure drop component that can be quite large at high heat and mass fluxes due to the small channel dimension. Since the outlet of the test section is kept near the atmospheric pressure, the local pressure at the location of thermocouples will become higher than the atmospheric pressure with increasing mass flux or quality due to a considerable pressure drop in mini-channels. The figures indicate that the new correlation can also predict saturated flow boiling heat transfer coefficients in mini-channels reasonably well. Fig. 7 shows the

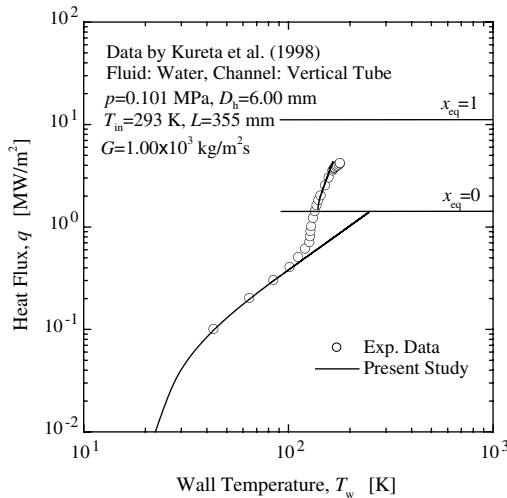


Fig. 6. Comparison with boiling curves at mass flux of $1000 \text{ kg/m}^2\text{s}$ [24].

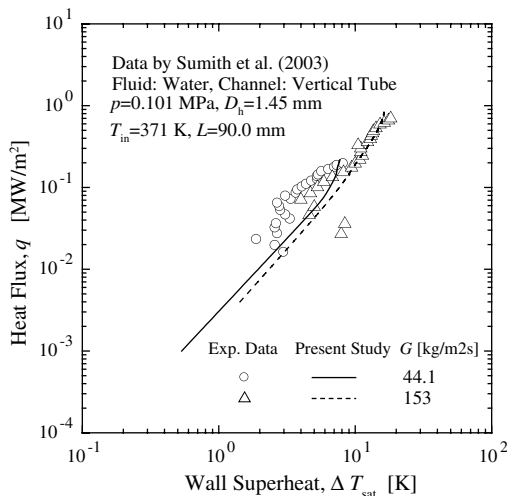


Fig. 7. Comparison with boiling curves by Sumith et al. [27].

comparison with boiling curves given by Sumith et al. in the saturated boiling regions. In both cases of mass flux, the prediction could agree well with the experiments data.

It should be mentioned here that since the original Chen correlation is applicable in the quality range of approximately 1–70%, the newly developed correlation should also obey this applicable range. As pointed out by Collier [34], the Chen correlation could be used in the subcooled region as well, if we use the following modifications:

$$q = S \cdot h_{nb}(T_w - T_{sat}) + F \cdot h_{sp}(T_w - T_b), \quad (1')$$

where $F = 1$ and $S = S(x_{eq} = 0)$. At extremely high quality, dryout will occur and the mechanism of heat transfer may be different. Application of the correlation may lose physical meaning in the very high quality region.

4. Conclusions

In view of practical importance of a heat transfer correlation for flow boiling, a generalized Chen correlation has been developed for saturated flow boiling heat transfer in mini-channels. The obtained results are as follows:

- (1) Existing general correlations and experimental studies related to saturated flow boiling heat transfer in mini-channels were extensively reviewed. An extensive database was collected for saturated flow boiling heat transfer in mini-channels under various experimental conditions such as different channel geometries (circular and rectangular), flow orientations (vertical and horizontal), and test fluids (water, R11, R12, and R113).
- (2) It was shown that a common feature of flow boiling heat transfer in many mini-channels is liquid-laminar and gas-turbulent flow. All existing correlations were developed for liquid-turbulent and gas-turbulent flow conditions, and thus it may be inconsistent to use them under other flow conditions in principle.
- (3) An extensive comparison of the existing correlations with the collected database shows that the Chen, the Liu–Winterton and the Kandlikar correlations work well for saturated flow boiling in mini-channels although physically they are not sound when liquid phase flow may be laminar.
- (4) It was found that the Reynolds number factor in the Chen correlation is proportional to the factor $\phi_{f,tt}$ for tt flow condition. A general form of the Chen correlation has been deduced for four flow conditions divided as Lockhart and Martinelli.
- (5) The generalized Chen correlation gave physically sound and good predictions for the four flow conditions, and can be recommended to predict saturated flow boiling heat transfer coefficients for mini-channels.

Acknowledgments

The authors would like to express their sincere appreciation to Drs. Y. Saito (Kyoto Univ.), X. Shen (Kyoto Univ.) and M. Kureta (JAERI) for their kind help. One of the authors (W. Zhang) gratefully acknowledges the

support by Japan Government (Monbukagakusho) Scholarship during his stay in Japan.

References

- [1] S.G. Kandlikar, Fundamental issues related to flow boiling in minichannels and microchannels, *Exp. Thermal Fluid Sci.* 26 (2002) 389–407.
- [2] S.S. Mehendale, A.M. Jacobi, R.K. Shan, Fluid flow and heat transfer at micro- and meso-scales with application to heat exchanger design, *Appl. Mech. Rev.* 53 (7) (2000) 175–193.
- [3] K. Mishima, T. Hibiki, Some characteristics of air–water two-phase flows in small diameter tubes, *Int. J. Multiphase Flow* 22 (4) (1996) 703–712.
- [4] K.A. Triplett, S.M. Ghiaasiaan, S.I. Abdel-Khalik, A. LeMouel, B.N. McCord, Gas–liquid two-phase flow in microchannels. Part I: Two-phase flow patterns, *Int. J. Multiphase Flow* 25 (1999) 377–394.
- [5] J.C. Chen, A correlation for boiling heat transfer to saturated fluid in convective flow, *ASME Paper*, 63-HT-34 (1963) 1–11.
- [6] M.M. Shah, A new correlation for heat transfer during flow boiling through pipes, *ASHRAE Trans.* 82 (2) (1976) 66–86.
- [7] S.S. Kutateladze, *Fundamentals of Heat Transfer*, Edward Arnold, London, 1963.
- [8] K.E. Gungor, R.H.S. Winterton, A general correlation for flow boiling in tubes and annuli, *Int. J. Heat Mass Transfer* 29 (1986) 351–358.
- [9] Z. Liu, R.H.S. Winterton, A general correlation for saturated and subcooled flow boiling in tube and annuli, *Int. J. Heat Mass Transfer* 34 (1991) 2759–2766.
- [10] S.G. Kandlikar, A general correlation for saturated two-phase flow boiling heat transfer inside horizontal and vertical tubes, *ASME J. Heat Transfer* 112 (1990) 219–228.
- [11] D. Steiner, J. Taborek, Flow boiling heat transfer in vertical tubes correlated by an asymptotic model, *Heat Transfer Eng.* 13 (2) (1992) 43–69.
- [12] W.M. Rohsenow, A method of correlating heat transfer data for surface boiling of liquids, *ASME Trans.* 74 (1952) 969–976.
- [13] A.E. Bergles, J.G. Collier, J.M. Delhaye, G.F. Hewitt, F. Mayinger, *Two-phase Flow and Heat Transfer in the Power and Process Industries*, Hemisphere Publishing Corp., 1981 (Chapter 8).
- [14] W.H. McAdams, *Heat Transmission*, second ed., McGraw-Hill, New York, 1942.
- [15] M.G. Cooper, Heat flow rates in saturated nucleate pool boiling—A wide-ranging correlation using reduced properties, *Adv. Heat Transfer* 16 (1984) 158–239.
- [16] V.E. Schrock, L.M. Grossman, Local heat transfer coefficient and pressure drop in forced convection boiling, UCRL-13062, University of California, Berkeley, 1957.
- [17] G.M. Lazarek, S.H. Black, Evaporative heat transfer, pressure drop and critical heat flux in a small diameter vertical tube with R-113, *Int. J. Heat Mass Transfer* 25 (7) (1982) 945–960.
- [18] K. Cornwell, P.A. Kew, Boiling in small parallel channels, in: *Proceedings of the International Conference on Energy Efficiency in Process Technology*, Elsevier Applied Science, 1992, pp. 624–638.
- [19] P.A. Kew, K. Cornwell, Correlations for prediction of boiling heat transfer in small-diameter channels, *Appl. Thermal Eng.* 17 (1997) 705–715.
- [20] M.W. Wambsganss, D.M. France, J.A. Jendrzejczyk, T.N. Tran, Boiling heat transfer in a horizontal small-diameter tube, *J. Heat Transfer* 115 (1993) 963–972.
- [21] T.N. Tran, M.W. Wambsganss, D.M. France, J.A. Jendrzejczyk, Boiling heat transfer in a small, horizontal, rectangular channel, in: *Heat Transfer, Atlanta AIChE Symp. Ser.* 89295, 1993, pp. 253–261.
- [22] T.N. Tran, M.W. Wambsganss, D.M. France, Small circular- and rectangular-channel boiling with two refrigerants, *Int. J. Multiphase Flow* 22 (3) (1996) 485–498.
- [23] W. Yu, D.M. France, M.W. Wambsganss, J.R. Hull, Two-phase pressure drop, boiling heat transfer, and critical heat flux to water in a small-diameter horizontal tube, *Int. J. Multiphase Flow* 28 (2002) 927–941.
- [24] M. Kureta, T. Kobayashi, K. Mishima, H. Nishihara, Pressure drop and heat transfer for flow-boiling of water in small-diameter tubes, *JSME Int. J., Ser. B* 41 (1998) 871–879.
- [25] Z.Y. Bao, D.F. Fletcher, B.S. Haynes, Flow boiling heat transfer of Freon R11 and HCFC123 in narrow passages, *Int. J. Heat Mass Transfer* 43 (2000) 3347–3358.
- [26] H.J. Lee, S.Y. Lee, Heat transfer correlation for boiling flows in small rectangular horizontal channels with low aspect ratios, *Int. J. Multiphase Flow* 27 (2001) 2043–2062.
- [27] B. Sumith, F. Kaminaga, K. Matsumura, Saturated flow boiling of water in a vertical small diameter tube, *Exp. Thermal Fluid Sci.* 27 (7) (2003) 789–801.
- [28] W. Qu, I. Mudawar, Flow boiling heat transfer in two-phase micro-channel heat sinks—I. Experimental investigation and assessment of correlation methods, *Int. J. Heat Mass Transfer* 46 (2003) 2755–2771.
- [29] R.W. Lockhart, R.C. Martinelli, Proposed correlation of data for isothermal two-phase two-component flow in pipes, *Chem. Eng. Prog.* 45 (1) (1949) 39–48.
- [30] H.K. Forster, N. Zuber, Dynamics of vapor bubbles and boiling heat transfer, *AIChE J.* 1 (4) (1955) 531–535.
- [31] D. Chisholm, A theoretical basis for the Lockhart–Martinelli correlation for two-phase flow, *Int. J. Heat Mass Transfer* 10 (1967) 1767–1778.
- [32] J.P. Hartnett, M. Kostic, Heat transfer to Newtonian and non-Newtonian fluid in rectangular ducts, *Adv. Heat Transfer* 19 (1989) 247–356.
- [33] H. Asaka, H. Ikawa, T. Maeda, M. Fukuchi, Y. Yabushita, K. Miyamoto, Safety analysis of upgraded JRR-3 by RETRAN-02/RR code (part 1) (Development of safety analysis code for research reactor), Japan Atomic Energy Research Institute, JAERI-M 84-217, 1984 (in Japanese).
- [34] J.G. Collier, *Convective Boiling and Condensation*, McGraw-Hill, London, 1972.